Waveguiding and nonlinear optical properties of three-dimensional waveguides in $LiTaO_3$ written by high-repetition rate ultrafast laser

Ben McMillen,[1] Kevin P. Chen,[1,a)] Honglin An,[2] Simon Fleming,[2] Vincent Hartwell,[3] and David Snoke[3]
[1]*Department of Electrical and Computer Engineering, University of Pittsburgh, Pittsburgh, Pennsylvania 15261, USA*
[2]*Optical Fibre Technology Centre, University of Sydney, Sydney, New South Wales 1430, Australia*
[3]*Department of Physics and Astronomy, University of Pittsburgh Pittsburgh, Pennsylvania 15261, USA*

(Received 28 May 2008; accepted 14 August 2008; published online 15 September 2008)

We report the fabrication of waveguides in lithium tantalate using a 250 kHz high-repetition rate ultrafast laser at 771 nm and the characterization of the resulting laser induced structure with second harmonic microscopy. Waveguides operating at the 1.5 μm telecommunication wavelength were formed above and below the focal volume using pulse energies ranging from 100 to 1.6 J and translation speeds from 100 μm/s to 5 mm/s. The second harmonic microscopy reveals no degradation of the electro-optic coefficient in the guiding region above the focal volume. © *2008 American Institute of Physics*. [DOI: 10.1063/1.2980437]

In the last decade, ultrafast lasers have emerged as a versatile tool for three-dimensional (3D) photonic circuit fabrication. Photonic components with increased complexity have been manufactured in a wide range of materials including silica-based glasses,[1,2] crystalline quartz,[3] and various nonlinear optical crystals such as lithium niobate.[4–7] The direct writing of embedded optical components in nonlinear crystals offers incentives to produce 3D active devices such as optical switches and routers to suit complicated optical network topologies. Fabrication of low-loss waveguides in crystalline materials is a challenge due to the anisotropic nature of the optical and mechanical properties of these materials, which are more susceptible to laser induced microcracks and optical scattering loss. In the last few years, low-loss waveguides have been produced by high repetition rate femtosecond laser pulses.[1,2] This is largely attributed to heat accumulation effects from pulse repetition rates of 250 kHz or greater, which enhances localized melting and thus assists in minimizing optical loss due to scattering. The high-repetition rate laser processing technique might be especially attractive for waveguide fabrication in crystalline materials as localized melting might reduce the anisotropic stress buildup around focal volume.[1]

The formation of index change regions by ultrafast laser irradiation involves multiple processes during the laser interaction with the writing medium. Laser-induced microexplosions produce voids and localized melting regions around the focal volume. The location, geometry, and magnitude of index change depend strongly on laser processing parameters as well as the properties of the physical writing medium. Using near-field optical microscopy and atomic force microscopy mapping, the index profiles induced in amorphous glasses have been extensively studied.[7] For nonlinear crystals and applications, the impact of laser-induced modification on nonlinear optical coefficients such as $\chi^{(2)}$ and $\chi^{(3)}$ must be considered simultaneously with the index change profile.

In this paper, we demonstrate for the first time, to our knowledge, the formation of high-quality waveguides through the use of a high repetition rate ultrafast laser in lithium tantalate ($LiTaO_3$). Further, waveguiding and electro-optic characteristics of the 3D waveguides are studied simultaneously around the laser modified regions.

Waveguide fabrication was performed using a Coherent MIRA oscillator and a RegA 9000 regenerative amplifier system, which produced 150 fs pulses at a wavelength of 770 nm and a repetition rate of 250 kHz. Waveguide inscription was possible at the fundamental wavelength of 770 and 385 nm through the use of a beta barium borate crystal for second harmonic (SH) generation. The output from this setup was then attenuated and passed through a 40× aspheric lens with a numerical aperture of 0.68. Samples were mounted on a three-axis computer-controlled linear motion stage (Aerotech AS32020) allowing precise control of the sample position in relation to the fixed lens focus. Z-cut $LiTaO_3$ was used for waveguide writing, which had a thickness of 0.5 mm. The writing beam was incident along the z-axis (c-axis) of the crystal and polarized parallel to the writing direction. Waveguide inscription was performed at a depth of 150 μm. Waveguides were formed using various pulse energies from 100 nJ to 1.6 μJ at 770 nm. Within this wide laser fluence window, 2.6 cm length waveguides were inscribed with writing speeds from 100 μm/s to 5 mm/s. The samples were then cut, ground, and polished for detailed characterization of each damage site.

With a wide laser processing window for waveguide fabrication in $LiTaO_3$, distinct guiding characteristics can be seen at the extremes of this range of parameters. Figures 1(a) and 1(b) show optical microscope pictures of the end-facet profile for damage sites created at 1.6 μJ (5 mm/s) and 300 nJ (1 mm/s), respectively. The laser beam was incident from the top of the image. Both laser fluences yield similar lateral waveguide width at ~1 μm. From this, we infer that the lateral width only depends on the focal spot size of the objective. This is in contrast to the ~2 μm waveguide width formed in fused silica using the identical optical setup and processing parameters. The 1 μm lateral width is just

a)Electronic mail: kchen@engr.pitt.edu.

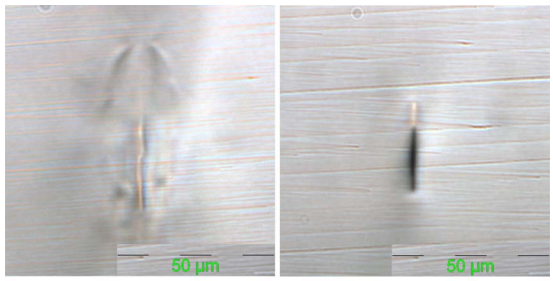

FIG. 1. (Color online) Optical microscope images of ultrafast laser induced material modifications for (a) 1.6 μJ at 5 mm/s and (b) 300 nJ at 1 mm/s.

slightly larger than the diffraction limit of the given objective (0.68 μm). The cross-sectional view of the modified region reveals significant differences between the two laser energies. The maximum available pulse energy of 1.6 μJ/pulse induces a much larger modified region than that caused by 300 nJ/pulse. Despite the higher energy, no visible voids were formed for this high fluence. In an interesting contrast, void regions became more prominent as the pulse energy was reduced to 300 nJ/pulse, which is visible as a dark strip approximately 20 μm long below the laser modified region, which was much more confined. For both pulse energies, a bright narrow strip appears to be the guiding region, although for higher energies guiding was found to exist outside this region. For the given conditions, the laser modified region extends much deeper into the $LiTaO_3$ than the depth of focus of the objective ($\sim$13 μm). The depths of visible laser damaged regions are $\sim$72 and $\sim$34 μm, respectively. This is in contrast to fused silica where the depth of the laser modified region roughly matches the depth of the focus of the objective.

Figures 2(b)–2(e) shows mode profile images captured using an IR charge-coupled device camera for the damage site pictured in Fig. 1(a) guiding 1550 nm. The waveguide was inscribed by 1.6 μJ/pulse at a writing velocity of 5 mm/s. The white-light image in Fig. 2(a) was taken with the same IR camera just before mode profile capturing and is given for reference so that the modes may be physically located within the laser-modified structure. The red scale bar in all figures represents a length of 15 μm. The large laser modified region induced at 1.6 μJ produced several guiding

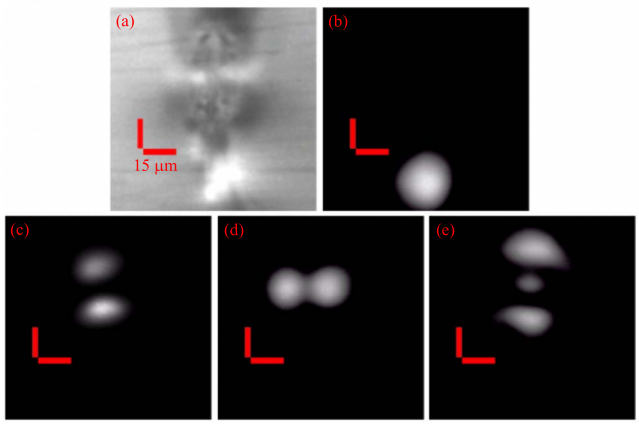

FIG. 2. (Color online) Layout of various guiding regions for the damage site written with 1.6 μJ at a velocity of 5 mm/s. The image in (a) is given as a reference. The scale bar in the image represents a distance of 15 μm.

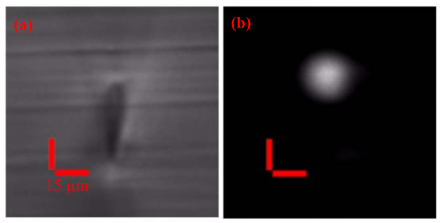

FIG. 3. (Color online) Guiding mode for the damage site written with 300 nJ at a velocity of 1 mm/s. The scale bar in the image represents a distance of 15 μm.

regions at 1550 nm. A well-defined single-mode guiding region appears below the laser modified region, as shown in Fig. 2(b). In contrast, guiding above the laser modified zone yields complex mode structures. By changing the launching condition, it was possible to couple into adjacent structures in the laser modified region, as shown in Figs. 2(c)–2(e). Due to the complexity of these structures, some of the observed modes may be higher order. Figures 3(a) and 3(b) show the guiding mode for the 300 nJ damage site written at 1 mm/s. For lower energies, guiding was found only to occur at regions just above the laser modified region. A single-mode waveguide appears to form with an average mode-field diameter of $\sim$20 μm. Figure 4 plots the mode-field diameter (MFD) as a function of laser writing speed for a pulse energy of 300 nJ. If the lateral size of 1 μm from the visual inspection shown in Fig. 1(b) is used as the waveguide size, the index change induced by the 300 nJ laser pulse is estimated to be $>1\times10^{-2}$. Single-mode guiding regions were formed for laser pulse energies less than 300 nJ for writing speeds between 100 μm/s to 1 mm/s.

In additional to the guiding properties, the modification of nonlinear optical properties of the laser modified area is equally important for device applications. The modification of the second-order nonlinearity (SON) was studied and visualized using SH microscopy. The microscope is equipped with dual photomultiplier transmitted light detectors to capture both the ordinary transmission optical images and SH images. A detailed description of the experimental setup can be found in Ref. 8. For microscopy specimen preparation, the Z-cut $LiTaO_3$ crystal with laser-written structures was affixed to a glass microscope slide for support and protection during sample grinding and polishing. Then the whole block was cleaved and the two exposed cross sections that were perpendicular to the lines of laser-written structures

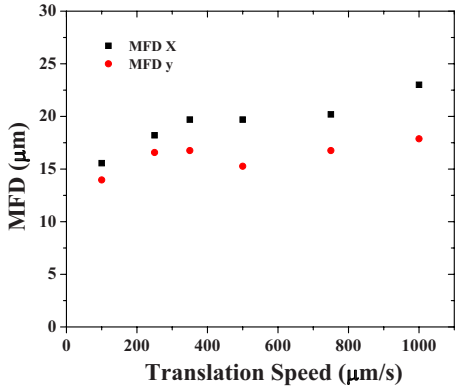

FIG. 4. (Color online) Plot of the corresponding X and Y MFDs for the 300 nJ site.

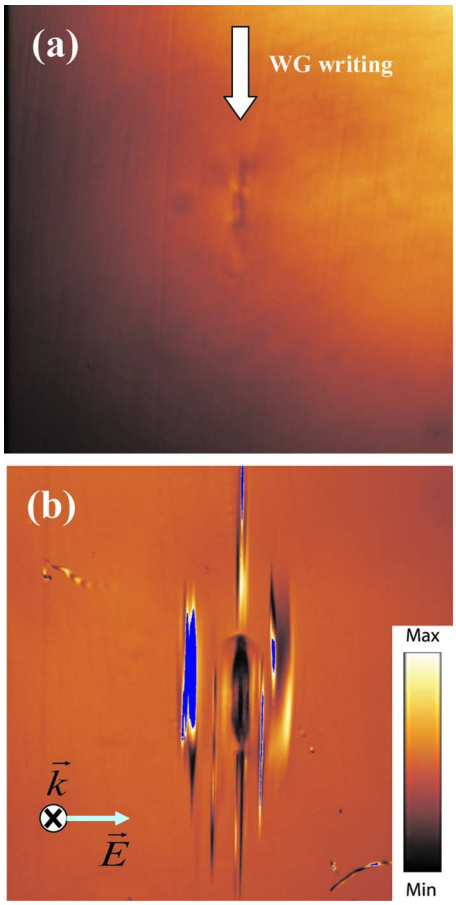

FIG. 5. (Color online) (a) Ordinary microscope picture of a laser modified region induced by 300 nJ laser pulse at 2 mm/s and (b) the SH image of the same site. The propagation direction and the polarization of incident YAG laser is indicated in the picture. The blue region indicate SH signal saturation.

were polished to an optical finish for the SH microscopy observation.

Figure 5(a) shows the ordinary transmission image of a waveguide cross section. A linearly polarized 830 nm Ti:sapphire laser was focused and scanned across the cross section of the waveguide. The resulting SH signal was collected to form the SH image of the waveguide, as shown in Fig. 5(b). The transverse spatial resolution of the SH microscopy was estimated to be $\sim 0.4\ \mu$m with a depth of focus $\sim 2\ \mu$m. Most of the SH signal was collected within the focal volume. The polarization of the incident fundamental beam was along the horizontal direction, as indicated in Fig. 5(b). It can be seen that within the focal volume, the SON has been significantly decreased, displaying a darker region compared to other parts of the sample. The edge of the SON-decreased region is rather smooth, suggesting a melting-and-resolidification process. The loss of SON within the focal volume indicates a destruction of the crystalline structure of the $LiTaO_3$ when irradiated by the high power femtosecond laser pulses. At the focal volume, the laser intensity is so high that nonlinear absorption occurs, transferring the laser energy to the crystalline structure and raising the temperature above the melting point of $LiTaO_3$. After the irradiation, the focal volume quickly cools down (within tens of microseconds) without recrystallization, thus losing original SON. This process should be accompanied by an increase in volume, creating stress around the focal volume. This effect could be account for the filamentary features observed around the focal volume in Fig. 5(b).

The SON decrease in the focal volume seems to be a drawback to the waveguide fabrication in $LiTaO_3$ through femtosecond pulse direct writing. However, as shown in Figs. 2 and 3, the waveguiding region actually lies above and below the focal volume. For the guiding region above the focal volume, we observe an approximately two times stronger SH signal than that collected from the background area without laser radiation. Even stronger SH signal was observed along both sides of the focal volume. The SH signal saturated the detector. Most of the SH signal was collected within focal volume with the depth of 2 μm, which is comparable to the coherence length of about 1.7 μm for the process of the SH generation. Thus the increase of the SH signal is unlikely due to the domain inversion of the crystal. On the other hand, the structure inhomogeneity and drastic index change induced by the ultrafast laser is likely the cause to the increase of the SH signal. Although the detailed mechanism of the SON changes is unknown, strong SH signal shown in Fig. 5(b) provides clear evidence that the guiding region retains crystalline structures and preserved strong SON coefficient. The result suggests that efficient nonlinear optical devices based such 3D waveguides can be fabricated using ultrafast lasers.

In summary, this paper reports guiding and electro-optic properties of waveguides in $LiTaO_3$ fabricated by ultrafast laser. Transmission experiment and SH microscopy confirms that waveguides operating at the telecommunication wavelength of 1.5 μm can be fabricated without the degradation of electro-optic coefficient of the crystal. The work demonstrates that high repetition rate ultrafast lasers can be a powerful tool to fabricate 3D active photonic circuits in nonlinear crystals.

This work is supported by National Science Foundation under awards of CMMI-0556086 and DMI0216785 and by the Australian Research Council under the Discovery funding scheme (DP0774404).

[1]S. Eaton, H. Zhang, P. Herman, F. Yoshino, L. Shah, J. Bovatsek, and A. Arai, Opt. Express **13**, 4708 (2005).
[2]H. Zhang, S. Eaton, J. Li, and P. Herman, J. Real Estate Res. **59**, 682 (2007).
[3]T. Gorelik, M. Will, S. Nolte, A. Tuennermann, and U. Glatzel, Appl. Phys. A: Mater. Sci. Process. **76**, 309 (2003).
[4]O. Beyer, I. Breunig, F. Kalkum, and K. Buse, Appl. Phys. Lett. **88**, 051120 (2006).
[5]J. Burghoff, C. Grebing, S. Nolte, and A. Tunnermann, Appl. Phys. Lett. **89**, 081108 (2006).
[6]A. Busacca, M. Cherchi, S. R. Sanseverino, A. C. Cino, A. Parisi, G. Assanto, M. Cichoki, F. Caccavale, D. Calleyo, and A. Morbiato, Fibres and Optical Passive Components, 2005. Proceedings of 2005 IEEE/LEOS Workshop, 2005 (unpublished), p. 126.
[7]L. Gui, B. Xu, and T. Chong Chong, IEEE Photonics Technol. Lett. **16**, 1337 (2004); S. Breer and K. Buse, Appl. Phys. B: Lasers Opt. **66**, 339 (1998).
[8]H. An, S. Fleming, and G. Cox, Appl. Phys. Lett. **85**, 5819 (2004).